frontiers | Frontiers in Earth Science

ORIGINAL RESEARCH
published: 12 May 2022
doi: 10.3389/feart.2022.857053

Characteristics and Accumulation Model of Silurian Tight Sandstone Gas Reservoir: A Case Study in the Shajingzi Belt, Northwest Tarim Basin, China

Yuanyin Zhang, Junfeng Zhang, Yongjin Gao, Yalei Liu, Miaoqing Miao, Qingyao Li and Zhichao Sun*

Oil and Gas Survey, China Geological Survey, Beijing, China

The first industrial gas flow has been recently achieved in the Shajingzi Belt, northwest Tarim Basin, China, although that area is always characterized as a monoclinic structure background, typical tight bituminous sandstones, and poor hydrocarbon accumulation conditions. Based on drilling, oil testing, geophysics, geological, and geochemical data, a comprehensive research including reservoir description, hydrocarbon tracing, and accumulation history analysis in the Shajingzi Belt was carefully conducted to establish a meaningful Silurian hydrocarbon accumulation model and discover potential areas in this study. It is found that 1) the Silurian reservoirs in the Shajingzi Belt mainly bear gas and could be defined as the typical tight sandstone reservoir with ultralow porosity generally less than 10% and low-permeability distributed between 0.1 and 10 mD, respectively; 2) petroleum substantially comes from the Cambrian–Ordovician source rocks, especially in the Awati Sag, possessing the dominant contribution from the shales in Cambrian Yuertusi Formation; 3) synthetically, three major hydrocarbon accumulation periods can be determined in the Shajingzi Belt, namely, the Late Caledonian, the Late Hercynian–Early Indosinian, and the middle Himalayan, respectively; 4) the evolution of Shajingzi Fault system apparently dominated the formation of various Silurian structural–lithologic traps in the monoclinic structure background and efficiently connected the deep source rocks in the Awati Sag, especially during Himalayan period when the current tight sandstone gas reservoirs were formed. This research could find its benefit for exploration in similar basin–range junction areas.

Keywords: tight sandstone gas, late hydrocarbon accumulation, structural traps, Silurian, Shajingzi Belt, Tarim Basin

OPEN ACCESS

Edited by:
Shang Xu,
China University of Petroleum (East China), China

Reviewed by:
Jin Lai,
China University of Petroleum, China
Ran Xiong,
PetroChina Hangzhou Research Institute of Geology, China

****Correspondence:***
Yuanyin Zhang
yuanyinshou@163.com

Specialty section:
This article was submitted to Economic Geology, a section of the journal Frontiers in Earth Science

Received: *18 January 2022*
Accepted: *12 April 2022*
Published: *12 May 2022*

Citation:
Zhang Y, Zhang J, Gao Y, Liu Y, Miao M, Li Q and Sun Z (2022) Characteristics and Accumulation Model of Silurian Tight Sandstone Gas Reservoir: A Case Study in the Shajingzi Belt, Northwest Tarim Basin, China. Front. Earth Sci. 10:857053. doi: 10.3389/feart.2022.857053

1 INTRODUTION

The Silurian bituminous sandstone reservoirs in the Tarim Basin, China, is widely distributed but has only submitted 3P oil reserves of 8011.97×10^4 t in Tazhong and Tabei areas until 2020 (Zhang et al., 2022). In particular, the hydrocarbon exploration degree in the northwest basin–range junction belt is comparably unsatisfactory. The geological condition and hydrocarbon accumulation in Tazhong and Tabei areas have been carefully discussed by previous research, which reveals the Silurian tidal

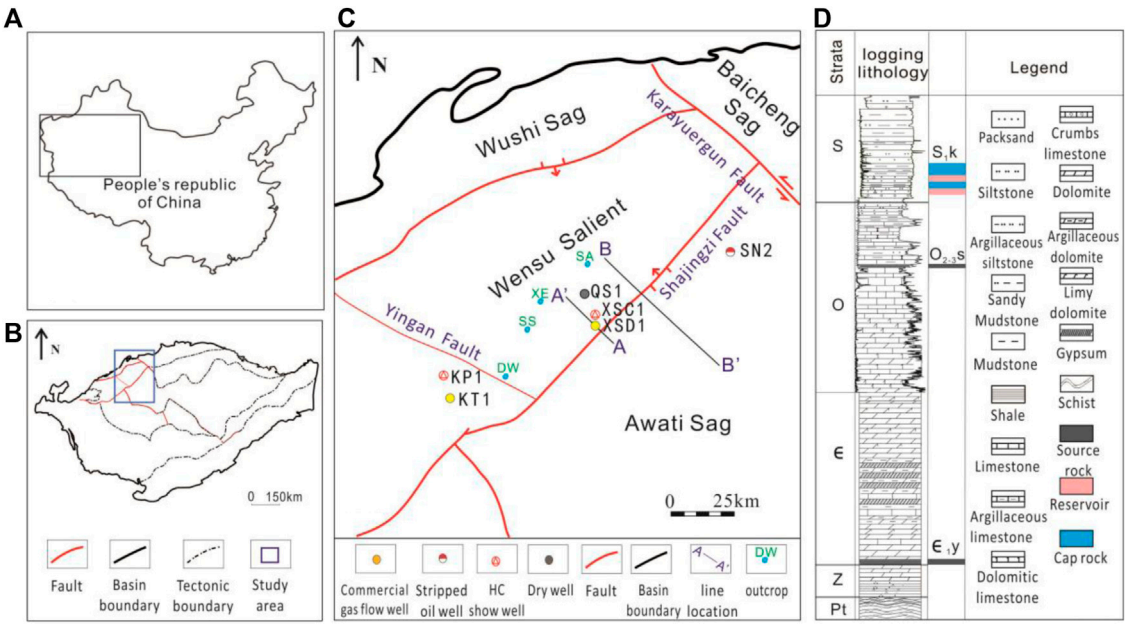

FIGURE 1 | Geological setting of the Shajingzi Belt in the northwest Tarim Basin. **(A)** Location of the Tarim Basin in China. **(B)** Location of the research area in the Tarim Basin. **(C)** Tectonic units of the Silurian in the Shajingzi tectonic belt, showing the sampling wells and outcrops. **(D)** Proterozoic lower palaeozoic lithology and source–reservoir–cap rock assemblage in the Shajingzi area, Keping Uplift (modified from Zhang et al., 2022).

flat sedimentary characteristics (Ding et al., 2012; Shang et al., 2016), bituminous sandstone reservoir types (Liu et al., 2000a; Liu et al., 2000b; Zhang et al., 2004; Zhu et al., 2005), and three primary reservoir-forming periods: Late Caledonian, Late Hercynian, and Yanshan–Himalayan (Lv et al., 2008; Zhang et al., 2011a; Hu et al., 2015). In addition, both the amount of oil and gas loss in the Late Caledonian (Jiang et al., 2008) and the bitumen issues for instance the ability of hydrocarbon preservation or secondary hydrocarbon generation were exploratory discussed (He et al., 2011).

By contrast, the Silurian tight sandstone reservoir in the Shajingzi Belt, northwest Tarim Basin, is always thought to be unqualified for efficient oil and gas preservation since the Lower Paleozoic strata often directly exposes in high-steep occurrence in that area (Wang et al., 2009; Li et al., 2013), although these outcrops undoubtedly made a great contribution for the primary Silurian stratigraphic division, lithology identification, and sedimentary formation analysis in the whole basin (Wang et al., 2007; Wu et al., 2011). However, Well XSD1 in 2018 drilled in the Shajingzi Belt resoundingly obtained industrial gas flow in the Silurian tight sandstone for the first time, and XSC1 in 2020 again obtained better oil and gas in the same Silurian layers (Zhang et al., 2020; Gao et al., 2021). Thus, both the tight sandstone reservoir characteristics and hydrocarbon accumulation model in the Shajingzi Belt require to be settled urgently, which is certainly beneficial for other complex basin–range junction belts by definition.

On the basis of drilling, oil testing, geophysical, and necessary reservoir geological and geochemical analyzing, integrating with structural evolution analysis, oil source correlation, and accumulation period determination, this study describes the tight reservoir properties in terms of mineralogy, morphology, porosity, and permeability and critically analyzes the petroleum characters, for instance, the quality, sourcing, and charging periods, thereby the Silurian hydrocarbon accumulation model in the Shajingzi Belt is constructed in the maximum reasonability.

2 GEOLOGICAL SETTING

The Shajingzi Belt is located in the southeast of Wensu salient, which is classified as the secondary tectonic unit in the northwest Tarim Basin and belongs to a typical basin–range junction belt (Zhang et al., 2022). It strikes in the northeast–southwest direction and was defined mainly by three boundary faults including the Karayuergun Fault in the north, the Yingan Fault in the south, and the Shajingzi Fault in the southeast, respectively (**Figure 1A–C**). The Shajingzi Fault accompanied with numerous secondary faults is regarded as the boundary between the Wensu Salient and the Awati Sag (Jia, 2005; Wang et al., 2009; Li et al., 2013; Qi et al., 2014; Zhang et al., 2022) (**Figure 1C**). Approximately, the fracture systems involve deep wedge-shaped thrusts, Shajingzi Fault in a narrow sense (painted in **Figure 2**), and shallow extensional faults as a whole (Li et al., 2013; Qi et al., 2014; Zhang et al., 2022).

Silurian in this area is often divided into four members: the upper Keziertag Formation ($(S_3\text{-}D_1)$k), the middle Yimugantawu Formation (S_2y), the lower Tata Ertag Formation (S_1t), and the Kepingtage Formation (S_1k), respectively (Wang et al., 2007; Wu et al., 2011; Zhang et al., 2022). As the most significant oil and gas

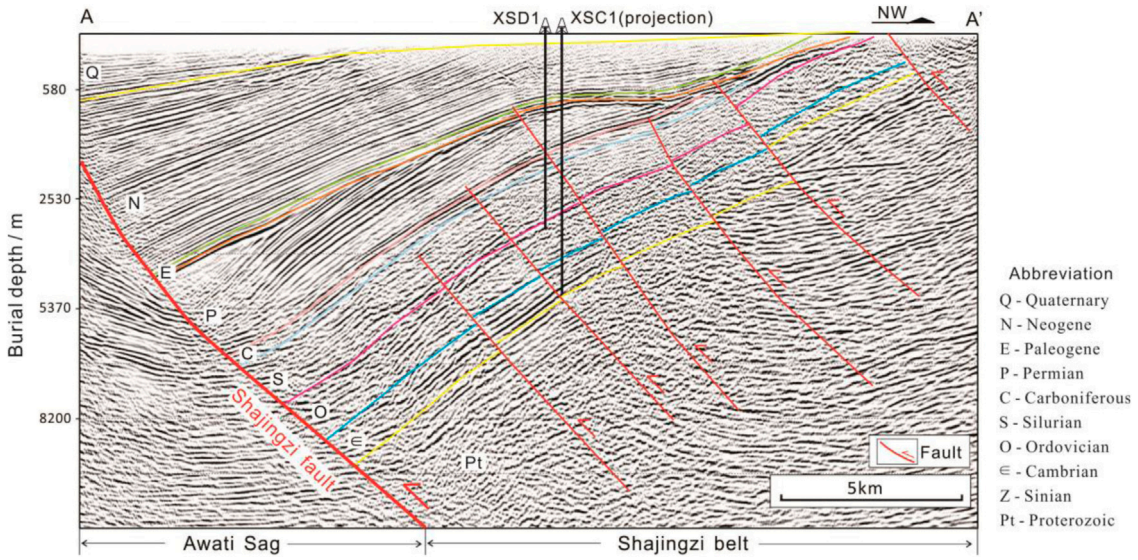

FIGURE 2 | Typical newest seismic section along the Shajingzi Fault in the study area (section locations are AA′ in **Figure 1C**).

bearing member, the Kepingtage Formation in particular is mainly composed of gray green and dark gray fine sandstone and argillaceous siltstone. Lower Paleozoic outcrops are commonly developed with considerable dip angles (30°–75°) in the west of the Shajingzi Belt, where the Silurian bituminous sandstone is conveniently surveyed in the Kepingtage Formation (S_1k), that is, the Sishichang and Dawangou outcrop profiles (Wu et al., 2011) (SS and DW outcrops in **Figure 1C**).

Mainly two sets of effective paleozoic marine source rocks were developed in the Shajingzi belt and Awati Sag, containing the calciferous black shale in the Saergan Formation, Ordovician ($O_{2\text{-}3}s$) and the silicon-containing black shale in the Yuertusi Formation, Cambrian (ϵ_1y), respectively (Gao et al., 2010; Zhang et al., 2012a; Xi et al., 2016). They are broadly exposed in the west of Shajingzi Belt that is, the Shiairike, Sishichang, Xiaoerbulak, and Dawangou outcrop profiles (Wu et al., 2011) (SA, SS, XE, and DW outcrops in **Figure 1C**, respectively).

Several NW-trending 2D seismic lines deployed during 1990–2003 (with fold times of 30) along the Shajingzi Fault are characterized as a poor imaging quality, yet they display a monoclinic background (rendered by the newest data in **Figure 2**) that is generally considered to be unbeneficial for hydrocarbon accumulation; thus, oil and gas exploration in this area was substantially short.

Based on the thorough re-conduction of two-dimensional seismic acquisition (with fold times of 1050) in the Shajingzi Belt from 2016 to 2018 (**Figure 2**), Well XSD1 was deployed in 2018 and triumphantly obtained Silurian industrial gas flow for the first time in the northwestern Tarim Basin (Zhang et al., 2020; Gao et al., 2021). According to the drilling, Kepingtage Formation (S_1k) can be further divided into three members: the interbeds of sandstone and mudstone in the up (S_1k_3), mudstone in the middle (S_1k_2), and sandstone and mudstone in the low (S_1k_1), respectively (**Figure 3**). In particular, a daily gas production of 1.2605×10^4 m^3 and water production of 16.38 m^3 were achieved at the interval of 2525.5–2528.5 m (S_1k_1), which was eventually concluded as a "water–gas layer." Another combined interval of 2377–2386 m and 2409–2413 m (S_1k_3) produced a daily gas production of 1.6817×10^4 m^3 and was finally concluded as a "gas layer." In addition, 2.16 m^3 of crude oil was successfully achieved in S_1k_3. In 2020, Well XSC1 encouragingly obtained better oil and gas show in the same layer of the Silurian, and additionally revealed both the Ordovician ($O_{2\text{-}3}s$) and Cambrian (ϵ_1y) source rocks at the rough burial depth of 2846–2861 m and 5074–5105 m, respectively.

3 MATERIALS AND METHODOLOGY

Forty-eight reservoir samples in Silurian were carefully selected for the thin section study from wells XSD1 and XSC1 and prepared by vacuum impregnation with blue epoxy resin to highlight pores. The intergranular pore-filling minerals and pore types can be identified via thin section observation. The samples were milled into ultrafine particles with sizes less than 40 μm. X-ray diffraction (XRD) was further performed to determine the mineralogy, by using a normal focus Cobalt X-ray tube used in a Siemens Diffractometer D8 at 40 mA and 40 kV. The porosity and permeability were systematically measured through placing sample plugs into a permeameter and injecting nitrogen at confining pressures of 100 psi and 400 psi.

A total of 26 oil-soaked/bituminous sandstone samples and 36 source rock samples from well XSD1, XSC1, and corresponding outcrops in the Shajingzi Belt were integrally selected for compound-specific carbon isotope analysis, which was carried out on a Micromass IsoPrime mass spectrometer attached to an HP 6890 GC (Li et al., 2010). Chromatographic separation by GC (Clarus 580 Perkin Elmer, MA, United States) and subsequent 34S/32S ratio measurements by a Neptune plus multi-collector inductively coupled plasma mass spectrometer (MC-ICPMS,

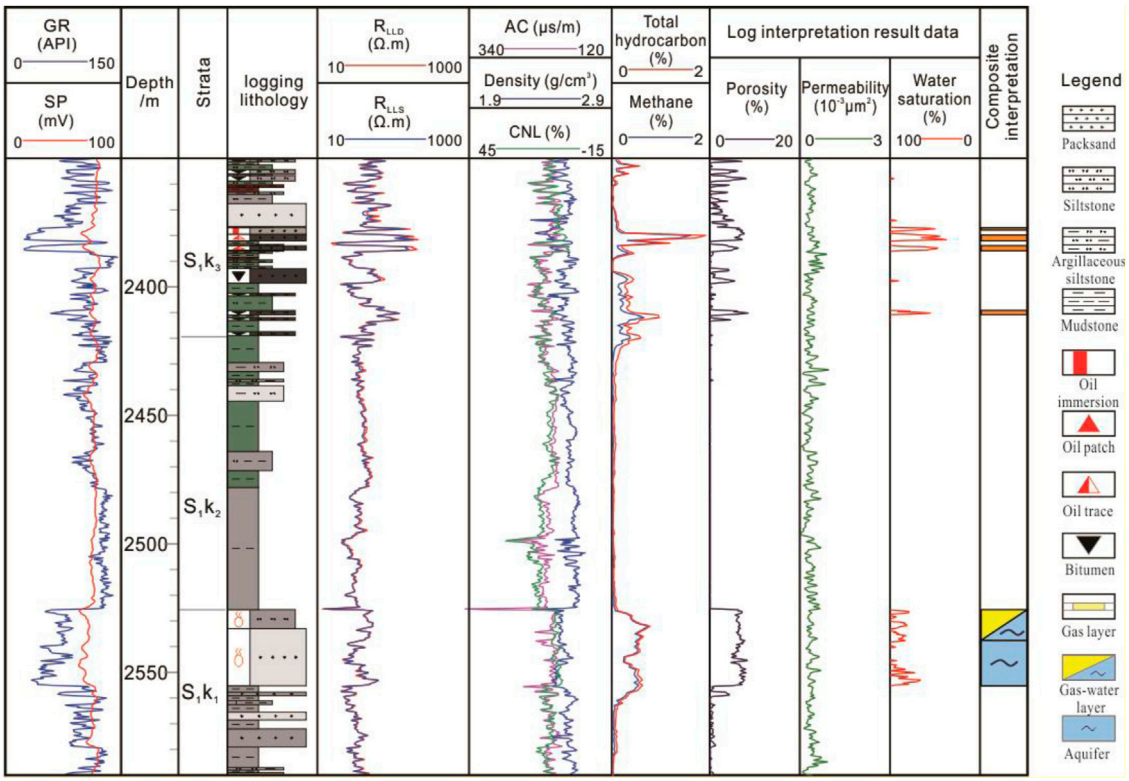

FIGURE 3 | Four-property diagram of Silurian Kepingtage Formation in Well XSD1.

Thermo Scientific, Bremen, Germany) (Li et al., 2015) were subsequently employed to analysis $\delta^{34}S$ values in individual compounds. The saturated hydrocarbons of 26 samples were thoroughly analyzed through the GC–MS (Agilent 7890-5975c GC–MS) to determine the relationship between the source rock and reservoirs. Both the sterane and terpane series characteristics were comprehensively studied by monitoring m/z 217 and m/z 191, respectively, in condition with appropriate comparison from the data in the Tazhong area. Seven Silurian oil–gas samples from well XSD1 and XSC1 were elaborately selected and made into polished thin sections preparing for fluid inclusion analysis. The fluid inclusion microthermometric analysis was carried out by using a Linkam THMS600 heating–freezing stage.

Based on data analysis of geochemical and geological characteristics in the studying area, combining with a 2D structural evolution research, the hydrocarbon accumulation model and evolution of Silurian tight sandstone gas reservoir in the Shajingzi Belt are comprehensively discussed.

4 RESULT AND DISCUSSION

4.1 Tight Sandstone Reservoir Characteristics

The paleogeographic pattern of the Tarim Block in the early Silurian was a westward opening gulf with the compound sedimentary system of tidal-dominated and tidal-flat facies

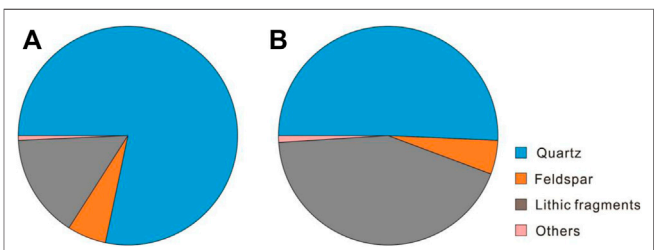

FIGURE 4 | Mineral composition of the tight sandstone gas reservoir in the Shajingzi Belt. **(A)** S_1k_1 is mainly quartz, lithic fragments, and feldspar; **(B)** S_1k_3 is mainly quartz and lithic fragments, following by feldspar.

(Zhang et al., 2022). Two periods of large tidal-dominated braided river deltas were, respectively, developed in the studying area during S_1k_1 and S_1k_3, and formed two sets of sandstone sedimentation (**Figure 3**). The sandstone reservoirs subsequently experienced complicated tectonic movements, and continuous compactions were further densified into tight sandstone gas reservoir. The measured mineral composition of the tight sandstone gas reservoir in the Kepingtage Formation is dominated by quartz and lithic fragments, where the averaging quartz content reaches to 78.3% in the S_1k_1 and 50.7% in the S_1k_3, and the averaging lithic content is 15.3% in the S_1k_1 and 43.3% in the S_1k_3, respectively (**Figure 4**). Feldspar is the third contributor with an average content of 5.7% in the S_1k_1 and 5% in the S_1k_3. The grain diameter of

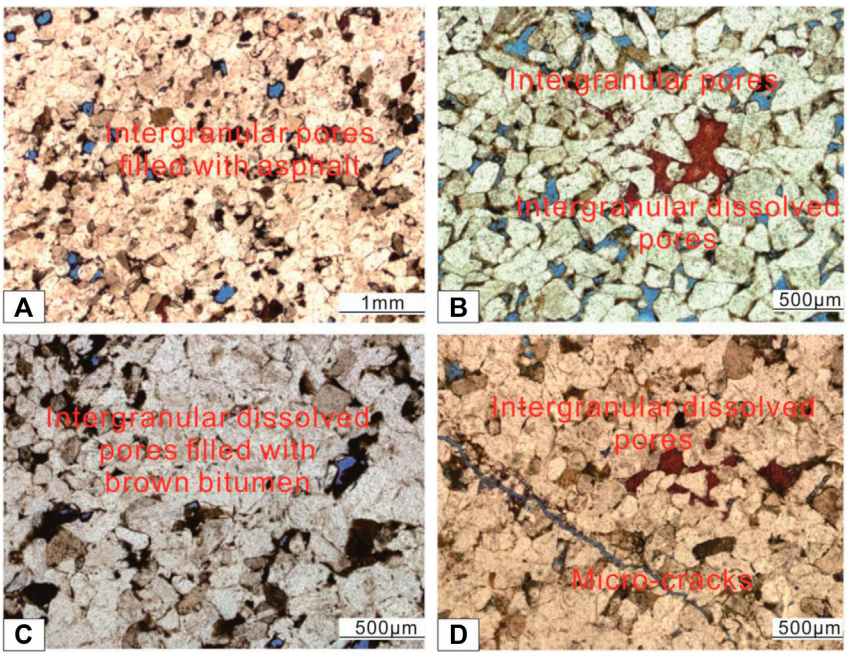

FIGURE 5 | Pore morphology of the typical tight sandstone gas reservoir in the Shajingzi Belt. **(A)** Well XSD1, 2380.77m, S_1k_3. **(B)** Well XSD1, 2381.92 m, S_1k_3. **(C)** Well XSD1, 2383.3 m, S_1k_3. **(D)** Well XSC1, 2373.45 m, S_1k_1.

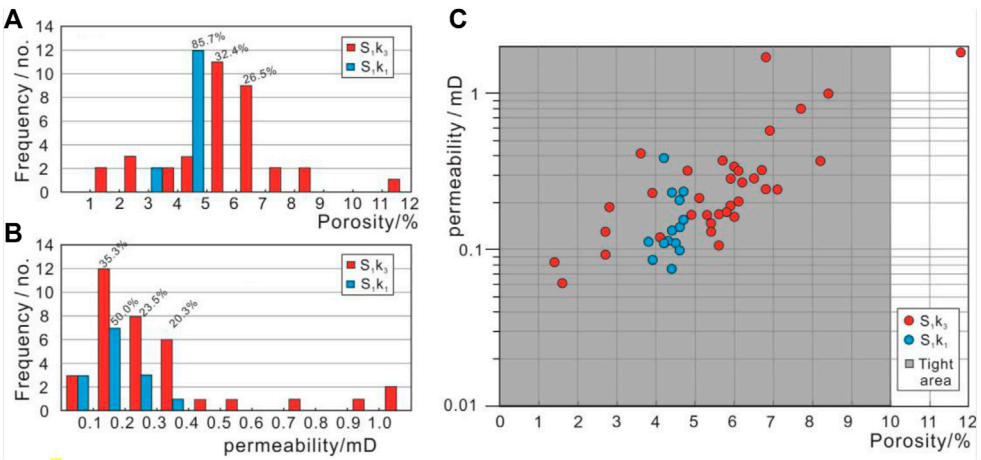

FIGURE 6 | Porosity and permeability distribution of the tight sandstone gas reservoir in the Shajingzi Belt. **(A)** Porosity. **(B)** Permeability. **(C)** Crossplot between porosity and permeability, while the shaded area mainly indicates the typical tight sandstone gas reservoirs.

clastic sandstone particles in both S_1k_1 and S_1k_3 is mainly distributed from medium to fine. The lithic is mainly constituted by quartzite and a small amount of igneous rock, supplementing with occasional occurrence of argillaceous, crystalline, and phyllite fragments.

The intergranular interstitial materials include argillaceous matrix, calcite, and secondary quartz. Calcite is characterized by medium-crystalline structure and plaque-like cemented particles. The pore type in this area is principally intergranular pores, followed by intergranular dissolved pores and a small

TABLE 1 | Analysis of natural gas samples from the Kepingtage Formation in Well XSD1.

Member	Depth/m	C_1/%	C_2/%	C_3/%	iC_4/%	nC_4/%	iC_5/%	nC_5/%	CO_2/%	N_2/%	Density/(g·cm^{-3})
S_1k_1	2 525.5–2 528.5	92.91	0.80	0.03	0.02	0.01	0.00	0.03	0.11	6.186	0.7053
S_1k_3	2 377.0–2 386.0 2 409.0–2 413.0	91.72	1.47	0.20	0.14	0.03	0.14	0.04	0.01	6.247	0.5958

amount of micro-cracks (**Figure 5**), while the pore diameter generally varies from 0.1 to 0.2 mm. Most of them are distributed in isolation with the strong heterogeneity. Some intergranular pores are filled by bitumen (**Figure 5A,C**). The throat is not commonly developed among the observed pores, demonstrating a poor connectivity as a whole.

The core samples overall exhibit poor reservoir properties in this area with the porosity ranging from 1.4% to 11.8% and *in situ* matrix permeability from 0.061 to 1.5 mD, respectively (**Figure 6**). The porosity of S_1k_1 varies from 3.8% to 4.7%, with an average value of 4.4%, while the permeability is distributed from 0.075 to 0.385 mD, with an average value of 0.157 mD. The porosity of S_1k_3 varies from 1.4% to 11.8%, with an average value of 5.4%, while the permeability is distributed from 0.061 to 1.5 mD, with an average value of 0.27 mD. Statistically, the tight sandstone gas reservoir in Kepingtage Formation can be characterized as ultralow porosity (<10%) and low permeability (0.1–10 mD) referring to the Chinese industrial standard (Jiang et al., 2015) (**Figure 6C**).

4.2 Petroleum Characteristics and Source Analysis

According to the oil testing result, both the S_1k_1 and S_1k_3 strata can be defined as atmospheric pressure formation with the measured pressure coefficient of 0.987 and 1.033, respectively. The natural gas compositions of the S_1k_1 and S_1k_3 in Well XSD1 are the same, with a relatively high content of methane and rare heavy hydrocarbon gas (**Table 1**). The obtained Silurian gas is further judged as dry gas referring to the large drying coefficient ($C_1/C_{1\text{-}5}$, 0.97–0.99). The C_1/C_2^+ value varies from 31.89 to 45.41. The light hydrocarbon heptane value is 30, and the paraffin index is 2, revealing the high maturity of natural gas. Thermal cracking at high temperature has not been traced from the comparison of carbon isotopic composition of methane and ethane.

The crude oil in the S_1k_3 is classified as conventional thin oil with modest density (0.8833 g/cm^3), low viscosity (16.98 mPa s at 50°C), and low wax content (3.4%), and its freezing point is 4°C. Crude oil group analysis exhibits the saturated hydrocarbon content varies from 52.87% to 72.65%, with an average value reaching 59.83%, while the aromatic hydrocarbons content distributed between 19.25% and 29.67%, with an average value of 22.43%. The averaging bitumen content of this crude oil is comparably high and reaches 9.92%, with the data distribution from 2.31% to 16.35%. Non-hydrocarbon is the fourth component, with content values from 5.80% to 11.36%. The obtained Silurian crude oil is essentially categorized as typical marine source referring to the relationship chart between DBT/P (dibenzothiophene/phenanthrene) and Pr/Ph ratio (0.78–0.85).

The regular sterane of crude oil in S_1k_3 is approximately characterized as high amplitudes in the right and low amplitudes in the left, showing a roughly asymmetric "V" shape in the partial m/z = 217 mass fragmentograms (**Figure 7**). The ratio of rearranged sterane and regular sterane varies from 0.21 to 0.27, while that between C_{30}-rearranged hopane and C_{30} hopane is limited from 0.10 to 0.13, implying relatively low rearranged sterane and C_{30}-rearranged hopane contents. In addition, the gammacerane index that varies from 0.13 to 0.15 is also comparably low.

The oil–oil correlation shows that Silurian oil from the Shajingzi Belt and that from the Tazhong area have similar geochemical characteristics (**Figure 7**), further indicating the similar geneses. In condition, both the saturated/aromatic hydrocarbon ratio (averaging 2.78) and non-hydrocarbon/bitumen ratio (averaging 1.32) in the Shajingzi Belt are similar to their counterparts in the Tazhong area, which possesses the corresponding average values of 2 and 1.49, respectively (Haijun et al., 2010). In particular, the Silurian oil in the Tazhong area is sourced from the mixture of Cambrian–Ordovician source rocks (Haijun et al., 2010).

On the other side, the Silurian oil obtained from well XSD1, XSC1 and Yuertusi Formation shale sampled from outcrops obviously exhibit closer isotope distributions and better affinity comparing with those of Ordovician Saergan Formation shale, especially in the sulfur isotope composition (**Figure 8**). Thus, we conclude that the Silurian crude oil substantially come from the mixture of Cambrian–Ordovician marine source rocks, yet possessing a more extensive contribution from Cambrian source rock.

4.3 Hydrocarbon Accumulation Discussion

4.3.1 Hydrocarbon Accumulation Time and Periods

(1) Free and adsorbed hydrocarbon: The total ion chromatogram (TIC) graph of gas chromatography/mass spectrometry of saturated hydrocarbons in Silurian oil in the Shajingzi Belt (**Figure 9**) distinctly shows that the paraffin is commonly developed, displaying an obvious hump of unresolved complex mixture (UCM) in the base line. This implies the secondary hydrocarbon charging existed after the degradation of initial by definition, which is comparably similar to that of Silurian crude oil in the Tazhong area (Haijun et al., 2010).

(2) Fluid inclusion analysis: Two major periods of homogenization temperature, including the distribution of 70°C–110°C and 140°C–170°C, respectively, were clearly determined by the temperature and pressure measurement in the Silurian tight sandstone reservoirs of Well XSD1 and XSC1. Petrography analysis of inclusions demonstrates that most observed fluid inclusions are roughly distributed along

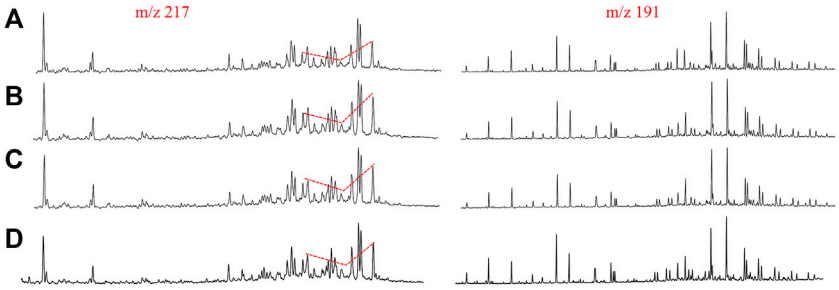

FIGURE 7 | Partial m/z = 217 and m/z = 191 mass fragmentograms of saturated hydrocarbon fractions from selected Silurian crude oil samples in the Shajingzi Belt and Tazhong area. **(A)** Well XSD1 in the Shajingzi belt, bituminous sandstone, 2358.25–2358.34 m. **(B)** Well XSD1 in the Shajingzi belt, oil-soaked bituminous sandstone, 2380.35–2380.47 m. **(C)** Well TZ47 in the Tazhong area, 4978.5–4986 m, crude oil. **(D)** Well TZ11 in the Tazhong area, 4301–4307 m, crude oil.

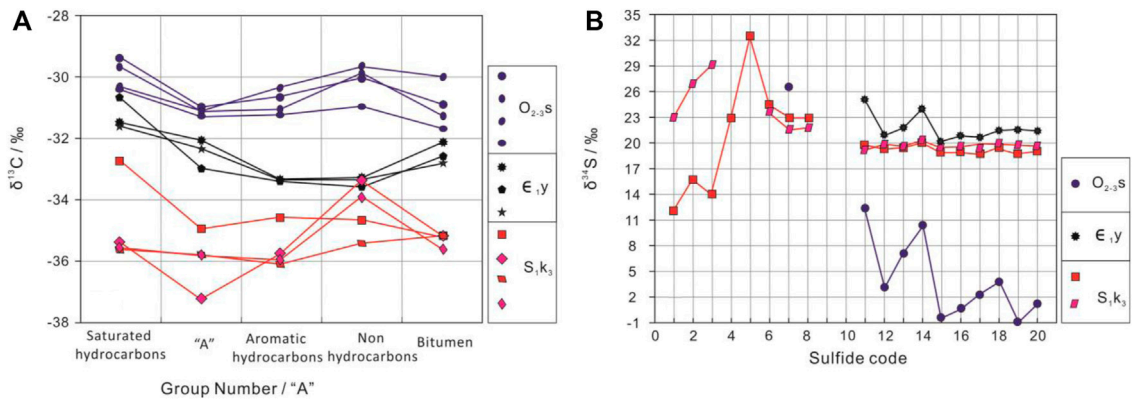

FIGURE 8 | Distribution features of the group component carbon isotopic **(A)** and sulfur isotopic **(B)** curves of the Silurian oil (S_1k_3) and Cambrian–Ordovician (ϵ_1y, $O_{2\text{-}3}s$) source rocks in the Shajingzi Belt.

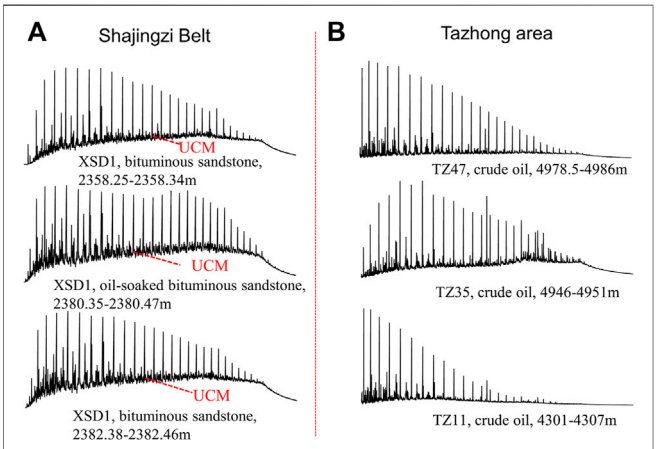

FIGURE 9 | Total ion chromatogram of the saturated fractions of selected Silurian samples from different wells in the Shajingzi Belt **(A)** and Tazhong area **(B)**.

the micro-fractures of quartz particles and highly formed during the early and middle stages of secondary enlargement of quartz grains in further. The major hydrocarbon charging period was then suggested to have happened during 410 Ma–430 Ma based on burial–thermal history comparison, when the hydrocarbon was relatively immature and characterized as yellow and green fluorescent colors (**Figure 10C**). The second charging was likewise to be determined at about 250 Ma. In addition, a younger hydrocarbon charging period roughly distributed during 32 Mpa is commonly observed from the similar Silurian experiments in the Tazhong and Tabei areas (Hu et al., 2015), which is also highly consistent with the local trap formation history (see **Section 4.3.2**). Overall, the absence of middle Himalayan fluid inclusion in our observations might be attributed to the limited number of Silurian oil–gas samples (only 7).

(3) Hydrocarbon generation history: As the most important Paleozoic source rock in the Tarim Basin, the silicon-containing black shale in the Yuertusi Formation, Cambrian (ϵ_1y) began to generate hydrocarbons in the Ordovician period. It reached the peak of initial oil generation during the Late Caledonian–Early Hercynian movement and the peak of gas generation during the mid-Himalayas movement, respectively (**Figure 11**) (Haijun et al., 2010; Li et al., 2015; Zhu et al., 2019). In comparison, the

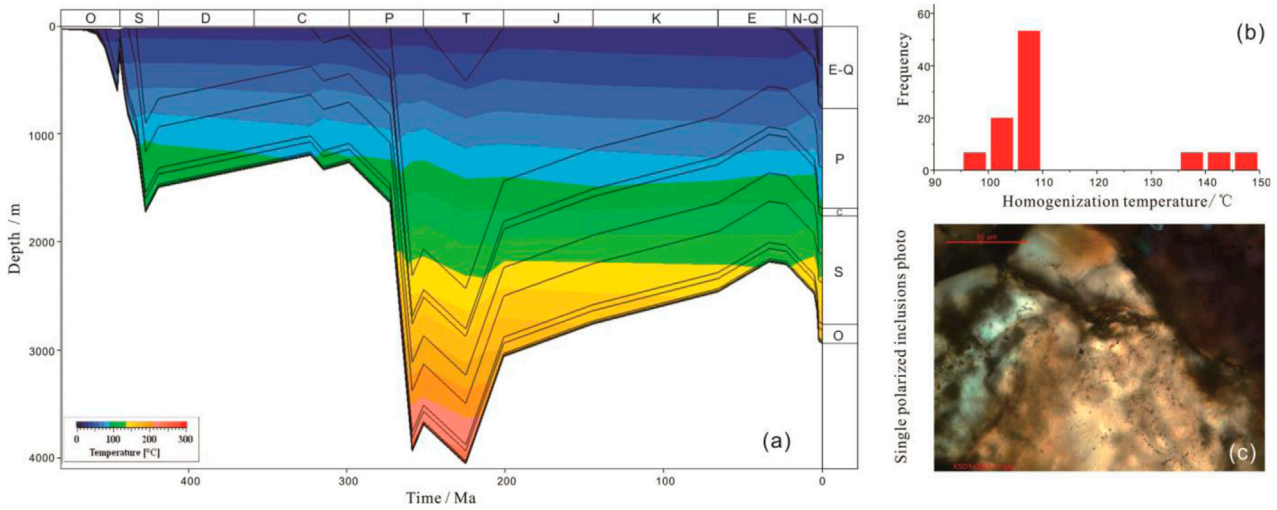

FIGURE 10 | Burial–thermal history and representative fluid inclusions characters of Well XSD1. **(A)** Burial–thermal history of Well XSD1; **(B)** homogenization temperature histogram of selected inclusions, Well XSD1, 2382.38m; **(C)** single polarized inclusions photo, Well XSD1, 2382.38 m.

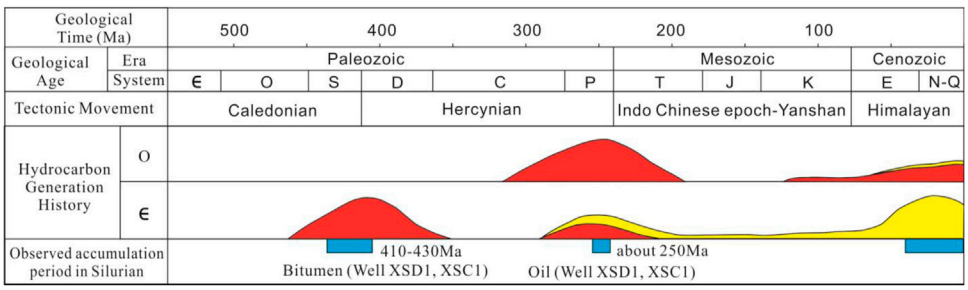

FIGURE 11 | Hydrocarbons generation from Paleozoic source rocks and tectonic evolution history in the Tarim Basin (modified from Li et al., 2015; and Zhu et al., 2019).

calciferous black shale in the Saergan Formation, Ordovician ($O_{2\text{-}3}s$), is widely considered to reach its peak of oil generation during the Late Hercynian–Early Indo-Chinese epoch–Yanshan movement (**Figure 11**) (Haijun et al., 2010; Li et al., 2015; Zhu et al., 2019). Apparently, the two hydrocarbon accumulation periods observed from fluid inclusion analysis in the Shajingzi Belt are well coupled with the oil generation peak time of Cambrian and Ordovician source rocks, respectively.

4.3.2 Tectonic Evolution and Trap Formation History

Basin–range junction areas are often characterized as complex tectonic activities, multiple trap types, rigorous sealing conditions, and complicated hydrocarbon accumulations. The Shajingzi fault was roughly shaped and comprised three major sets: the deep wedge-shaped thrusts, Shajingzi Fault in a narrow sense, and shallow extensional faults, respectively (Wang et al., 2009; Li et al., 2013; Qi et al., 2014; Zhang et al., 2022). On the basis of the latest 2D seismic data along the Shajingzi Fault with a better image of the Paleozoic strata (**Figure 2**), tectonic evolution analysis from the Awati Sag to Shajingzi Belt is thoroughly conducted. The Shajingzi Fault was internally activated by the uplift of Wensu Salient since the end of the Ordovician (**Figure 12A**) and gradually formed wedge-shaped thrusts between the Shajingzi Belt and Awati Sag until the Late Caledonian–Early Hercynian movement (**Figure 12B**). Subsequently, the upper plate of Shajingzi Fault zone was consistently uplifted and gradually formed the prototype of the fault belt and early structural traps till the end of the Permian (**Figure 12C**), which also caused the significant stratigraphic dip increase in Lower Paleozoic strata. This process was slightly weakened but continued to form the Shajingzi Fault system in a narrow sense till the end of Miocene epoch when the Silurian traps were finally shaped (**Figure 12D**).

After that, the extensional faults were further developed in the Pliocene-Quaternary (**Figure 12E**). On the whole, Silurian traps in the Shajingzi Belt, that are mainly structural types such as fault blocks, fault noses, and anticlines, are dominated by the Shajingzi

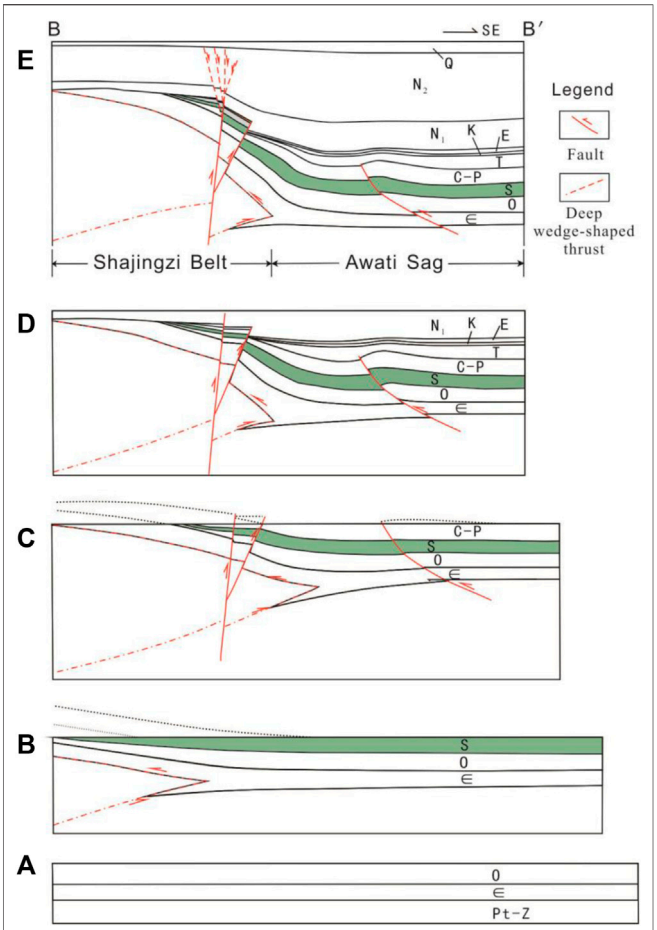

FIGURE 12 | Tectonic evolution profile between the Shajingzi Belt and Awati Sag at key geology periods (modified from Qi et al., 2014) (section is mapped in **Figure 1C**, and the strata abbreviation refers to **Figure 2**). **(A)** Pre-Silurian: tectonic stabilization period. **(B)** Pre-Carbonaceous: forming the deep thrust wedge. **(C)** Pre-Triassic: forming the prototype of the fault belt and early structural traps. **(D)** Pre-Pliocene: finalization of the Shajingzi fault in a narrow sense and corresponding traps. **(E)** Current section.

Fault system in essence, which was developed in a large scale and could efficiently connect the deep source rocks in the Awati Sag.

4.3.3 Hydrocarbon Accumulation Evolution and Model

Based on the integral comparison of hydrocarbon generation history of Cambrian–Ordovician source rocks and Silurian trap evolution history of the Shajingzi Belt, multiple periods of hydrocarbon accumulation in the Silurian reservoirs, primarily including the Late Caledonian–Early Hercynian, Late Hercynian, and Himalayan in particular can be ultimately examined. In detail, the primary process of the Silurian hydrocarbon accumulation and evolution in the Shajingzi Belt is simulated as follows:

(1) Initial hydrocarbon accumulation period: The Shajingzi Belt was gradually uplifted and separated from the Awati Sag starting from the Late Caledonian when the Silurian deposited sand bodies merely suffered insufficient diagenesis and overburden issues. Thus, the Silurian reservoir in that time apparently possessed superior physical properties and was apt to form tremendous traps. These traps were probably filled with normal oil since the source rock of the Cambrian Yuertusi Formation reached the oil generation peak as well in the same period, which could be migrated through the initial fault system (**Figure 13A**).

(2) Initial reservoir degradation period: In the Early Hercynian period, the South Tianshan Ocean fiercely subducted northward and the Tarim Basin was extensively uplifted as a whole (Jia, 2005; Li et al., 2013). The Silurian–Devonian generally suffered denudation, inevitably resulting in intensive degradation of initial Silurian oil reservoirs and extensive formation of bituminous sandstone in the Kepingtage Formation (Lv et al., 2008; Zhang et al., 2011a). Initial Silurian oil reservoirs restricted in some deep favorable structural positions might be limitedly remained during this process, yet the corresponding crude oil still became heavier (**Figure 13B**).

(3) Secondary hydrocarbon accumulation period: The uplift rate of Shajingzi Belt become increasingly fast since Carboniferous and approximately arrived at the maximum at Late Triassic, which

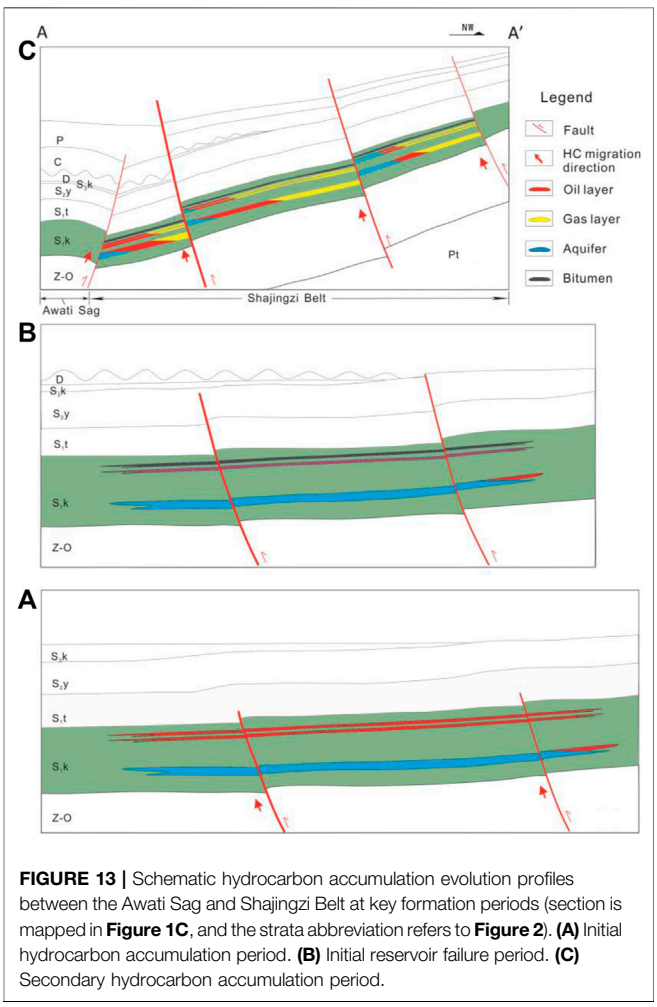

FIGURE 13 | Schematic hydrocarbon accumulation evolution profiles between the Awati Sag and Shajingzi Belt at key formation periods (section is mapped in **Figure 1C**, and the strata abbreviation refers to **Figure 2**). **(A)** Initial hydrocarbon accumulation period. **(B)** Initial reservoir failure period. **(C)** Secondary hydrocarbon accumulation period.

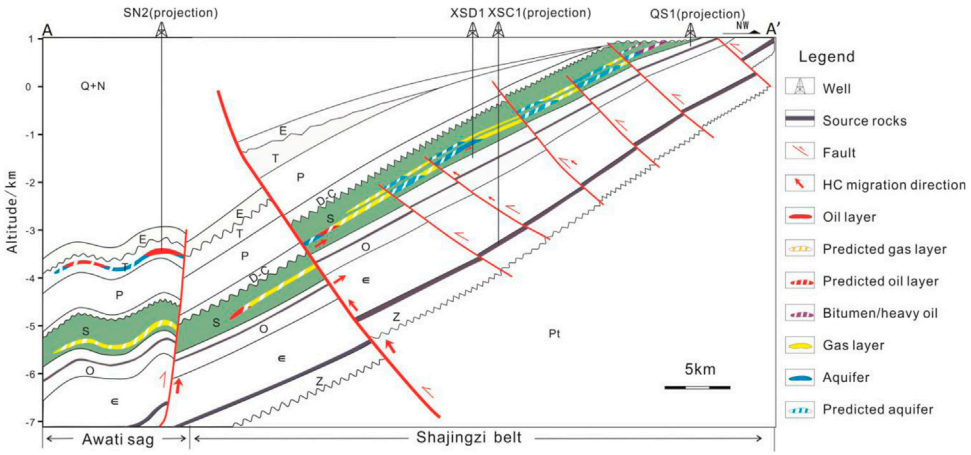

FIGURE 14 | Reservoir model between the Awati Sag and Shajingzi Belt (section location is AA′ in **Figure 1C**, and the strata abbreviation refers to **Figure 2**).

gradually generated the monoclinic structure background and prototype if Silurian structural–lithological traps. Meanwhile, the black shale in the Saergan Formation, Ordovician reached the initial oil production peak during the Late Hercynian–Early Indosinian, while the Cambrian Yuertusi Formation also produced plenty of natural gas. Undoubtedly the oil and gas could be efficiently migrated into Silurian traps through the Shajingzi Fault systems; therefore, this could be apparently attributed to the secondary hydrocarbon accumulation period. Nevertheless, the Shajingzi Belt continued to be uplifted after this movement, so those traps continued to experience multifarious adjustments and resulted to a substantial loss of the secondary charged hydrocarbons (**Figure 13C**).

(4) Tertiary hydrocarbon accumulation period: The Shajingzi Fault displacement between Shajingzi Belt and Awati Sag still increased after Triassic, yet possibly in a slower speed and lighter intensity. This process was speculated to be gradually reduced and completely stopped until the middle Himalayan period, which inevitably further decorated and finalized the previous Silurian structural–lithological traps and corresponding reservoirs. Meanwhile, the source rock in the Cambrian Yuertusi Formation was in the stage of gas generation peak during that period. Thus, although Silurian reservoirs in the Shajingzi Belt possibly become comparably tight because of intensive diagenesis and complex tectonic compression, considerable gas could still migrate along the fault system, unconformity, and sand bodies into Silurian traps to finally form the current distribution of oil and gas reservoirs, which is characterized by gas preponderance (**Figure 14**).

Therefore, the Silurian reservoir model (**Figure 14**) in the Shajingzi Belt is apparently controlled by structure feature and principally charged in the Himalayan movement, since the Silurian structural or structural–lithological traps were completely finalized until mid-Himalayan period, and the current reservoir revealed by drilling in the Shajingzi Belt is mainly characterized as gas. The Shajingzi Fault was developed in a large scale and has a comparably long active time starting from the early Silurian and stopped in middle Neogene, accompanied with a series of induced faults in the Shajingzi Belt. The whole fault systems not only essentially controls the formation and distribution of Silurian structural and structural–lithological sandstone traps in the Shajingzi tectonic belt but also efficiently connected the hydrocarbon sourced from the Cambrian–Ordovician shales during key accumulation periods, primarily including Late Caledonian, Late Hercynian-Early Indosinian, and Himalayan. The basin–range junction belt is always characterized as complex structural activities and hydrocarbon accumulation history, yet might be also enriched in oil and gas as long as the trap formation and hydrocarbon charging are well matched and efficiently connected. In particular, the late accumulation especially in the middle Himalayan period might be a common phenomenon for the basin–range junction area in the Tarim Basin, considering the hydrocarbon generation and trap evolution histories (Zhang et al., 2011b; Zhang et al., 2012b). The current Silurian reservoirs are dominated by fault blocks (revealed by Well XSD1 and XSC1) and sequentially distributed along the tectonic belt. On the slope background of the Shajingzi tectonic belt, hydrocarbon sealed by the overlying mudstone caprock and lateral faults within each fault blocks tend to be rich in the structural high parts of Silurian sandstones (**Figure 14**). Anticline reservoirs might be developed beneath the footwall of Shajingzi Fault (well SN2 encountered crude oil in Triassic at the burial depth at about 6200 m). Stratigraphic reservoirs corresponding to the Silurian unconformity might be developed but are more susceptible to be degraded because of the poorer preservation.

5 CONCLUSION

The Silurian tight sandstone gas reservoirs in the Shajingzi Belt, northwest Tarim Basin, China, normally characterized as ultralow porosity (<10%) and low permeability (0.1–10 mD), could be extensively developed, and effectively enriched in hydrocarbon, although they historically suffered complicated diagenesis and

intensive tectonic activities and currently placed in a monoclinic background with an average dip of 30°. Silurian hydrocarbon in the Shajingzi Belt is speculated to be primarily derived from the deep Cambrian–Ordovician source rocks and dominated by the shales in Cambrian Yuertusi Formation. The Shajingzi fault system with a large scale has definitely controlled the traps formation and distribution; also, it consistently provides an efficient pathway for hydrocarbon migrated from deep source rocks. Three typical hydrocarbon charging periods were determined comprehensively: the Late Caledonian, the Late Hercynian–Early Indosinian, and the middle Himalayan movements, respectively. The current hydrocarbon model in the Shajingzi Belt is related to the structure pattern in essence, suggesting the general significance of late hydrocarbon accumulation in basin–range junction areas.

DATA AVAILABILITY STATEMENT

The original contributions presented in the study are included in the article/Supplementary Material, further inquiries can be directed to the corresponding author.

AUTHOR CONTRIBUTIONS

Methodology, integral research and analyzing, and writing: YZ; supervision and investigation: JZ and YG; structural analysis: YL; and material preparation, drawing, and editing: MM, QL, and ZS.

FUNDING

This research was financially funded by China Geological Survey Projects (DD20190106, DD20190708, DD20221674 and DD20190090).

ACKNOWLEDGMENTS

The authors thank doctor Ronghu Zhang from the Research Institute of Petroleum Exploration and Development, professor Xiaofeng Liu from China University of Geosciences, and professors Sumei Li and Zezhang Song from China University of Petroleum-Beijing for their significant suggestions.

REFERENCES

Ding, M., Fan, T., Gao, Z., and Li, R. (2012). Sedimentary Facies Analysis of the Lower Bitumen-Bearing Sandstone-Member of Kepingtage Formation, Silurian in Tazhong Area,Tarim Basin. *Geoscience* 26 (2), 342–348. doi:10.3969/j.issn.1000-8527.2012.02.015

Gao, Y., Zhang, J., Zhang, Y., Zhou, X., Bai, Z., Yang, Y., et al. (2021). The First Silurian Commercial Gas Flow Obtained by Well XSD1 in the Northwest Tarim Basin. *Geology. China* 48 (5), 1655–1656. doi:10.12029/gc20210525

Gao, Z., Zhang, S., Li, J., Zhang, B., Gu, Q., and Lu, Y. (2010). Distribution and Sedimentary Environments of Saergan and Yingshan Shales of the Middle-Uppler Ordovician in Western Tarim Basin. *J. Palaeogeogr.* 12 (5), 599–608. doi:10.7605/gdlxb.2010.05.009

Haijun, Y., Sumei, L., Xiongqi, P., Zhongyao, X., Qiaoyuan, G., and Baoshou, Z. (2010). Origin of the Silurian Crude Oils and Reservoir Formation Characteristics in the Tazhong Uplift. *Aata Geologica Sinca* 84 (5), 1128–1140. doi:10.1111/j.1755-6724.2010.00285.x

He, K., Mi, J., Zhang, S., and Wang, X. (2011). Secondary Hydrocarbon Generation of the Silurian Asphalt sandstone in the Tarim Basin and its Geological Implication. *Oil&gas Geology.* 32 (54), 682–691. doi:10.11743/ogg20110506

Hu, J., Wang, T., Chen, J., Su, J., Cui, J., Zhang, B., et al. (2015). Source Recognition and Charging Analysis of Oil in the Silurian Bituminous sandstone in the Tarim Basin: Evidences from Biomarker Compounds. *Nat. Gas Geosci.* 26 (5), 930–941. doi:10.11764/j.issn.1672-1926.2015.05.0930

Jia, C. (2005). Foreland Thrust-fold belt Features and Gas Accumulation in Midwest China. *Pet. Exploration Develop.* 32 (4), 9–15. doi:10.3321/j.issn:1000-0747.2005.04.002

Jiang, Z.-X., Li, Z., Li, F., Pang, X.-Q., Yang, W., Liu, L.-F., et al. (2015). Tight sandstone Gas Accumulation Mechanism and Development Models. *Pet. Sci.* 12 (4), 587–605. doi:10.1007/s12182-015-0061-6

Jiang, Z., Pang, X., Liu, L., Wang, X., Zhang, J., and Li, H. (2008). Quantitative Study of the Destroy Hydrocarbon Resource of the Silurian Bituminous sandstone in the Tarim Basin. *Chin. Sci. Bull.* 38 (Suppl. p), 89–94. doi:10.3321/j.issn:1006-9267.2008.z1.011

Li, S., Amrani, A., Pang, X., Yang, H., Said-Ahmad, W., Zhang, B., et al. (2015). Origin and Quantitative Source Assessment of Deep Oils in the Tazhong Uplift, Tarim Basin. *Org. Geochem.* 78 (6), 1–22. doi:10.1016/j.orggeochem.2014.10.004

Li, S., Pang, X., Jin, Z., Yang, H., Xiao, Z., Gu, Q., et al. (2010). Petroleum Source in the Tazhong Uplift, Tarim Basin: New Insights from Geochemical and Fluid Inclusion Data. *Org. Geochem.* 41 (6), 531–553. doi:10.1016/j.orggeochem.2010.02.018

Li, Y., Sun, L., Yang, H., Zhang, G., Qi, Y., Sang, H., et al. (2013). The Late Cenozoic Tensor-Shear Fault Zones Around Awati Sag, NW Tarim Basin. *Chin. J. Geology.* 48 (1), 109–123. doi:10.3969/j.issn.0563-5020.2013.01.006

Liu, L., Zhao, J., Zhang, S., Fang, J., and Xiao, Z. (2000a). Genetic Types and Characteristics of the Silurian Asphaltic Sandstones in Tarim Basin. *Acta Petrolei Sinica* 21 (6), 12–17. doi:10.3321/j.issn:0253-2697.2000.06.002

Liu, L., Zhao, J., Zhang, S., Fang, J., and Xiao, Z. (2000b). The Depositional and Structural Settings and the Bituminous sandstone Distribution Characters of the Silurian in Tarim Basin. *Acta Sedimentologica Sinica* 22 (6), 11–17. doi:10.3321/j.issn:0253-2697.2001.06.003

Lv, X., Bai, Z., and Zhao, F. (2008). Hydrocarbon Accumulation and Distributional Characteristics of the Silurian Reservoirs in the Tazhong Uplift of the Tarim basin. *Earth Sci. Front.* 15 (2), 156–166. doi:10.3321/j.issn:1005-2321.2008.02.018

Qi, Y., Li, Y., Wang, Y., Liu, Y., Zhu, H., Liu, Li., et al. (2014). Fault Analysis on Shajingzi Structural belt, NW Margin of Tarim Basin, NW China. *Chin. J. Geology.* 47 (2), 265–277. doi:10.3969/j.issn.0563-5020.2012.02.001

Shang, K., Guo, N., and Zhang, R. (2016). Sedimentary Facies of the Lower Bitumen-Bearing sandstone Member of the Silurian Kepingtage Formation I Nthe S1 Well Area, Tarim Basin. *Sediment. Geology. Tethyan Geology.* 36 (4), 14–20. doi:10.3969/j.issn.1009-3850.2016.04.003

Wang, C., Zhang, H., Li, Y., and Shen, Y. (2007). Stratigraphic Division, Correlation and Geologic Significance of Silurian in Tarim Basin. *Xinjiang Pet. Geology.* 28 (2), 185–188. doi:10.3969/j.issn.1001-3873.2007.02.015

Wang, G., Li, Y., Sun, J., Huang, Z., Zhao, Y., and Liu, Y. (2009). Structural Deformation Characteristics of the Kalpin Thrust belt, NW Tarim. *Chin. J. Geology.* 44 (1), 50–62. doi:10.3321/j.issn:0563-5020.2009.01.005

Wu, L., Jiao, Y., and Rong, H. (2011). Sedimentary Characteristics of Silurian Kepingtage Formation Bituminous sandstone at Sishichang Section, Western Tarim Basin. *Geoscience* 25 (1), 48–54. doi:10.3969/j.issn.1000-8527.2011.01.006

Xi, Q., Yu, H., Gu, Q., Qian, L., Li, X., and Li, S. (2016). Main Hydrocarbon Source Rocks and Contrasts for Awati Sag in Tarim Basin. *Pet. Geology. Oilfield Develop. Daqing* 35 (1), 12–18. doi:10.3969/J.ISSN.1000-3754.2016.01.003

Zhang, J., Pang, X., Liu, L., Jiang, Z., and Liu, Y. (2004). The Distribution Characteristics and Geological Meanings of the Silurian Bituminous sandstone in the Tarim Basin. *Chin. Sci. Bull.* 34 (Suppl. p), 169–176. doi:10.3321/j.issn:1006-9267.2004.z1.020

Zhang, J., Zhang, Y., and Gao, Y. (2022). Silurian Hydrocarbon Exploration Breakthrough in the Shajingzi Structural belt of Northwest Tarim Basin and its Implications. *Pet. Exploration Develop.* 9 (1), 233–246. doi:10.1016/S1876-3804(22)60019-3

Zhang, S., Gao, Z., Li, J., Zhang, B., Gu, Q., and Lu, Y. (2012a). Identification and Distribution of marine Hydrocarbon Source Rocks in the Ordovician and Cambrian of the Tarim Basin. *Pet. Exploration Develop.* 39 (3), 285–293. doi:10.1016/s1876-3804(12)60046-9

Zhang, S., Zhang, B., Yang, H., Zhu, G., Su, J., and Wang, X. (2012b). Adjustment and Alteration of Hydrocarbon Reservoirs during the Late Himalayan Period, Tarim Basin, NW China. *Pet. Exploration Devepment* 39 (6), 668–679. doi:10.1016/s1876-3804(12)60096-2

Zhang, S., Zhang, B., Li, B., Zhu, G., Su, J., and Wang, X. (2011a). History of Hydrocarbon Accumulations Spanning Important Tectonic Phases in marine Sedimentary Basins of China: Taking the Tarim Basin as an Example. *Pet. Exploration Develop.* 38 (1), 1–15. doi:10.1016/S1876-3804(11)60010-4

Zhang, Y., Zhang, Z., Feng, X., Su, X., Song, H., and Wu, X. (2011b). Main Controlling Factors and Models of Silurian Hydrocarbon Accumulation in the Southern Tahe Oilfield. *Acta petrolei Sinica* 32 (5), 767–773. doi:10.7623/syxb201105005

Zhang, Y., Gao, Y., Bai, Z., Jiang, K., Yang, Y., Han, M., et al. (2020). New Hydrocarbon Discoveries via XSD1 Drilling in the Eastern Keping Uplift, Tarim Basin. *Geology. China* 47 (6), 1930–1931. doi:10.12029/gc20200628

Zhu, G., Zhang, Z., Zhou, X., Li, T., Han, J., and Sun, C. (2019). The Complexity, Secondary Geochemical Process, Genetic Mechanism and Distribution Prediction of Deep marine Oil and Gas in the Tarim Basin, China. *Earth-Science Rev.* 198 (6), 1–28. doi:10.1016/j.earscirev.2019.102930

Zhu, R., Guo, H., He, D., Gao, Z., Lup, P., Wang, X., et al. (2005). Sand Bodies and Their Reservoir Quality in the Silurian Kepingtage Formation in Tazhong Area, Tarim Basin. *Pet. Exploration Develop.* 32 (5), 16–24. doi:10.3321/j.issn:1000-0747.2005.05.003

Conflict of Interest: The authors declare that the research was conducted in the absence of any commercial or financial relationships that could be construed as a potential conflict of interest.

Publisher's Note: All claims expressed in this article are solely those of the authors and do not necessarily represent those of their affiliated organizations, or those of the publisher, the editors, and the reviewers. Any product that may be evaluated in this article, or claim that may be made by its manufacturer, is not guaranteed or endorsed by the publisher.